HeI Photoelectron and Valence Synchrotron Photoionization Studies of the Thioester Molecule CH 3 C(O)SCH 3 : Evidence of Vibronic Structure

ARTICLE *in* THE JOURNAL OF PHYSICAL CHEMISTRY A · AUGUST 2008

Impact Factor: 2.69 · DOI: 10.1021/jp801295g · Source: PubMed

7 AUTHORS, INCLUDING:

Anthony J Downs
University of Oxford
258 PUBLICATIONS **5,062** CITATIONS
SEE PROFILE

Mauricio Federico Erben
National University of La Plata
90 PUBLICATIONS **795** CITATIONS
SEE PROFILE

Mao-Fa Ge
Chinese Academy of Sciences
259 PUBLICATIONS **3,011** CITATIONS
SEE PROFILE

Carlos O. Della Vedova
National University of La Plata
293 PUBLICATIONS **2,676** CITATIONS
SEE PROFILE

HeI Photoelectron and Valence Synchrotron Photoionization Studies of the Thioester Molecule $CH_3C(O)SCH_3$: Evidence of Vibronic Structure

Mariana Geronés,[†] Anthony J. Downs,[‡] Mauricio F. Erben,[†] Maofa Ge,[§] Rosana M. Romano,[†] Li Yao,[§] and Carlos O. Della Védova*,[†,||]

CEQUINOR (CONICET-UNLP), Departamento de Química, Facultad de Ciencias Exactas, Universidad Nacional de La Plata, C. C. 962 (1900) La Plata, República Argentina, Laboratorio de Servicios a la Industria y al Sistema Científico (LaSeISiC), UNLP-CIC-CONICET, Camino Centenario e/ 505 y 508, (1903) Gonnet, República Argentina, Inorganic Chemistry Laboratory, University of Oxford, South Parks Road, Oxford OX1 3QR, U.K., and State Key Laboratory for Structural Chemistry of Unstable and Stable Species, Beijing National Laboratory for Molecular Sciences (BNLMS), Institute of Chemistry, Chinese Academy of Sciences, Beijing 100080, People's Republic of China

Received: February 13, 2008; Revised Manuscript Received: April 17, 2008

One of the simplest thioester molecules, S-methyl thioacetate, $CH_3C(O)SCH_3$, has been investigated by HeI photoelectron spectroscopy (PES) and valence photoionization studies using synchrotron radiation in the same energy range. In the second series of experiments, total ion yield (TIY), photoelectron photoion coincidence (PEPICO), and partial ion yield (PIY) spectra were recorded. It was found that the photodissociation behavior of $CH_3C(O)SCH_3$ can be divided into three well-defined energy regions. Vibronic structure was observed in the valence synchrotron photoionization process, being associated with wavenumbers of 912, 671, 1288, 1690, and 1409 cm^{-1} for the bands at 12.82, 13.27, 15.66, 15.72, and 17.42 eV, respectively. Evaluation of the PE spectrum in concert with the synchrotron photoionization measurements and complemented by high-level ab initio calculations thus provides unusually detailed insights into the valence ionization processes of this molecule.

Introduction

Thioesters of the type RC(O)SR′ occur naturally in a variety of environments. Bacterial metabolism of methanethiol, CH_3SH, leads to the generation of a range of sulfur compounds that are present in various dairy products.[1,3] Significant contributions to the aroma of cheese, for example, comefrom not only dimethyl di- and trisulfides, but also some thioesters such as $CH_3C(O)SCH_3$ and $C_3H_7C(O)SCH_3$.[2,3] Thioesters have also been identified as being among the sulfur compounds that contribute to the aroma of wines.[4] In recognition of sensory properties that are quite pronounced at very low concentrations, a combinatorial approach has been used to build up a "flavor library" for S-methyl thioesters and other volatile sulfur compounds.[5] In vivo, thioesters result from the association of a methanethiol moiety and acyl coenzyme A via spontaneous or enzymatically promoted reactions.[6,7] This fact, along with the biochemical importance of coenzyme A and its acyl derivatives, has ensured the maintenance of a lively interest in thioesters.[8,10] Analysis of the different reactivities of thioesters and oxoesters has played a significant part, for example, in aiding our understanding of the driving force for acetylation reactions of coenzyme A.[11]

S-Methyl thioacetate, $CH_3C(O)SCH_3$, is thus a naturally occurring flavoring agent,[12] first synthesized in 1939 by Arndt et al. by the reaction of $CH_3C(O)Cl$ with CH_3SH.[13] The molecule has been characterized on the basis of its vibrational[14,15] and NMR[16] spectra. The structure of the gaseous molecule has been determined by gas electron diffraction (GED) with the assistance of quantum chemical calculations (B3LYP/6-31G* and MP2/6-31G*), thus establishing that it has a syn conformation (i.e., in relation to the C═O and S—CH_3 bonds).[8] Earlier quantum chemical studies included semiempirical[17] and ab initio[18] calculations. A recent report detailed a complete conformational analysis including solvent effects, with the derived parameters applied to the parametrization of a force field for the molecular modeling of unusual proteins containing an acylated cysteine side chain.[19] Matrix experiments involving the isolation of the vapor in solid Ar at 15 K have shown that irradiation with broadband UV−visible light results in hydrogen abstraction from the methyl group of the $CH_3C(O)$ function to give ketene, $H_2C{=}C{=}O$, with the elimination of CH_3SH as the main channel of photodecomposition (eq 1)[20]

$$CH_3C(O)SCH_3 \xrightarrow{h\nu} H_2C{=}C{=}O + CH_3SH \qquad (1)$$

We recently started a general project aimed at elucidating the shallow and inner-shell core electronic properties of sulfenyl carbonyl derivatives, XC(O)SY, and hence gaining a fuller understanding of the photodissociation channels open to these compounds. Thus, we have carried out photoionization studies on species such as FC(O)SCl,[21,22] ClC(O)SCl,[23] thioacetic acid [$CH_3C(O)SH$],[24] and $CH_3OC(O)SCl$[25] using synchrotron radiation in the range of 100−1000 eV. These studies involved measurements of not only the total ion yield (TIY) and partial ion yield (PIY) spectra, but also multicoincidence spectra [photoelectron−photoion coincidence (PEPICO) and photoelectron−photoion−photoion coincidence (PEPIPICO)] around the main ionization edges. The recent development of a neon gas filter

* To whom correspondence should be addressed. E-mail: carlosdv@quimica.unlp.edu.ar.
† Universidad Nacional de La Plata.
‡ University of Oxford.
§ Chinese Academy of Sciences.
|| UNLP-CIC-CONICET.

10.1021/jp801295g CCC: $40.75
Published on Web 06/11/2008

in the TGM line at the Brazilian Synchrotron National Laboratory (LNLS) now affords "pure" synchrotron radiation in the 12−21.5 eV range, and this has allowed us to expand the study of photoionization processes into the valence region. The combination of PES and multicoincidence time-of-flight- (TOF-) based techniques seems to offer a most promising approach to a deeper understanding of the electronic structure and the ionic dissociation induced by photon absorption in the valence region.

Herein, we report a study of the photon impact excitation and ionization dissociation dynamics of S-methyl thioacetate, $CH_3C(O)SCH_3$, in a combined approach that includes the use of HeI photoelectron spectroscopy and photoionization under the action of synchrotron radiation in the valence region. Total and partial ion yields were measured, together with the PEPICO spectra at selected photon energies, thereby allowing the study of the dissociation dynamics of excited $CH_3C(O)SCH_3$ molecules. A significant feature is the observation of vibrationally resolved progressions in the synchrotron-based spectroscopy.

Experimental Section

Synchrotron radiation from the Brazilian Synchrotron Light Source (LNLS) was used.[26] Linearly polarized light monochromatized by a toroidal grating monochromator (available at the TGM beam line in the range of 12−310 eV)[27] intersected the effusing gaseous sample inside a high-vacuum chamber at a base pressure in the range of 10^{-8} mbar. During the experiments, the pressure was maintained below 2×10^{-6} mbar. The intensity of the emergent beam was recorded by a light-sensitive diode. The photon energy resolution from 12 to 21.5 eV was given by $E/\Delta E = 550$. The ions produced by the interaction of the gaseous sample with the light beam were detected by means of a time-of-flight (TOF) mass spectrometer of the Wiley−MacLaren type for PEPICO measurements. This instrument was constructed at the Institute of Physics, Brasilia University, Brasilia, Brazil.[28] The axis of the TOF spectrometer was perpendicular to the photon beam and parallel to the plane of the storage ring. Electrons were accelerated to a multichannel plate (MCP) and recorded without energy analysis. This event started the flight-time determination process for the corresponding ion, which was subsequently accelerated to another MCP. High-purity vacuum-ultraviolet photons were used, the problem of contamination by high-order harmonics being suppressed by the innovative gas-phase harmonic filter recently installed at the TGM beam line at the LNLS.[29,30]

The HeI PE spectrum of $CH_3C(O)SCH_3$ was recorded on a double-chamber UPS-II machine built specifically to detect transient species at a resolution of about 30 meV, as indicated by the $Ar^+(^2P_{3/2})$ photoelectron band.[31–37] Experimental vertical ionization energies (I_v in electronvolts) were calibrated by simultaneous addition of a small amount of argon and iodomethane to the sample.

OVGF[38] calculations using the 6-311++G(d,p) basis set and B3LYP/6-311++G(d,p)-optimized geometry of the syn conformer were performed on $CH_3C(O)SCH_3$ in its ground electronic state using the Gaussian 03 program package.[39] The energies of dissociation of the $CH_3C(O)SCH_3^+$ parent ion into possible fragments were calculated at the UB3LYP/6-311++G** level of approximation.

The sample of S-methyl thioacetate, $CH_3C(O)SCH_3$, was obtained from a commercial source (Aldrich, 95%). The liquid was purified by fractional distillation and subsequently purified further by repeated fractional condensation at reduced pressure in order to eliminate volatile impurities. The final purity of the compound in both the vapor and liquid phases was carefully checked by reference to the following spectra: IR (vapor), Raman (liquid), and ^{13}C NMR (liquid).[8,14,16]

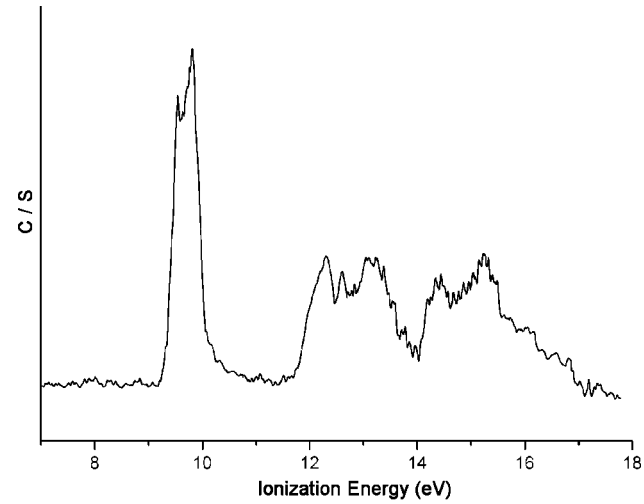

Figure 1. HeI photoelectron spectrum of $CH_3C(O)SCH_3$.

TABLE 1: Experimental and Calculated Ionization Energies and MO Characters for $CH_3C(O)SCH_3$

PES (eV)	calcd (eV)[a]	MO	character	TIY (eV)	VS (cm^{-1})[b]
9.53	9.35	24	n''(S)	−	
9.81	10.29	23	n'(O)	−	
12.25	12.28	22	$\pi''_{C=O}$	12.82	912 ± 43
12.64	13.37	21	σ_{C-H}(C=O)		
13.17	13.82	20	σ_{C-H}(C=O)	13.27	671 ± 147
14.63	15.03	19	σ_{C-H}(C=O)	15.66	1288 27 > 36
	15.09	18	σ_{C-H}(SCH_3)	15.72	1690 ± 80
15.23	15.86	17	σ_{C-H}(SCH_3)	16.99	
	16.22	16	σ_{C-H} (SCH_3)		
	16.53	15	σ_{S-C}(SCH_3)	17.42	1409 ± 40
	18.55	14	σ_{S-C} (C=O)	17.69	
		13	n'_oS	18.04	

[a] Values calculated at the OVGF/6-311++G(d,p) level of approximation with B3LYP/6−311++G**-optimized geometries. [b] VS indicates bands with vibronic structures observed in the TIY spectrum.

Results and Discussion

The molecule $CH_3C(O)SCH_3$ in the ground electronic state belongs to the C_s point group. It follows that all canonical molecular orbitals of type a′ are σ orbitals (in-plane), whereas those of type a″ are π orbitals. The 30 valence electrons are then arranged in 15 doubly occupied orbitals in the independent particle description. The photoelectron spectra, as well as the dissociative photoionization and the photoion branching ratios of $CH_3C(O)SCH_3$, are conveniently discussed with reference to this ground-state configuration.

Photoelectron Spectra. The HeI PE spectrum of $CH_3C(O)SCH_3$ is depicted in Figure 1. The experimental and theoretical ionization energies are listed in Table 1. Assignments were made with reference to the results of the OVGF/6-311++G(d,p) calculations [with an optimized geometry for the syn conformer at the B3LYP/6-311++G(d,p) level of approximation]. The characters of the 12 highest occupied molecular orbitals of $CH_3C(O)SCH_3$ are shown in Figure 2.

The first ionization band appearing in the spectrum at 9.53 eV can be assigned with confidence to the ionization process from the HOMO, an n''(S) orbital, which can be visualized as a lone pair nominally localized on the sulfur atom. Vertical ionization energies for the related species FC(O)SCl,

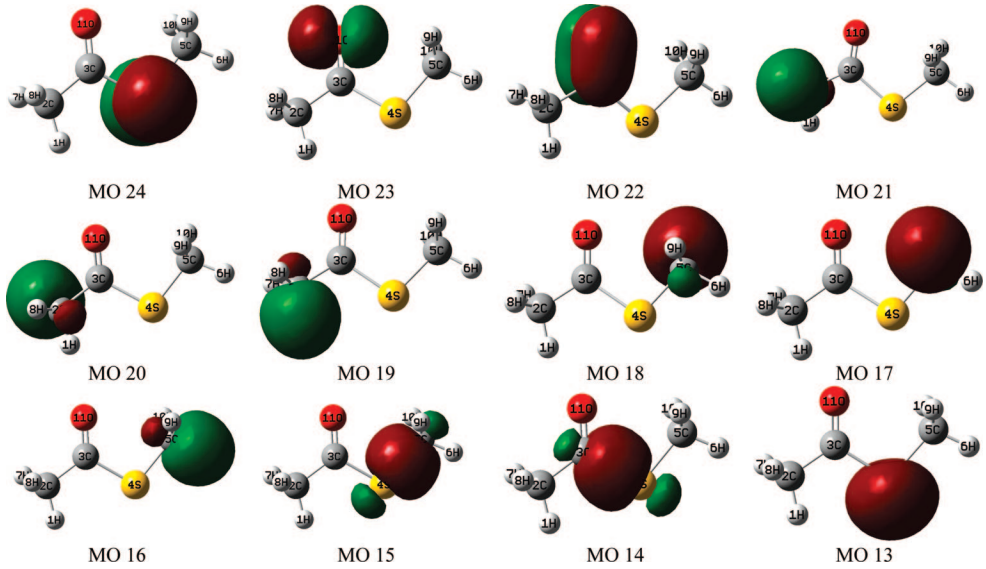

Figure 2. Characters of the 12 highest occupied molecular orbitals of $CH_3C(O)SCH_3$. The trend following Table 1 is from MO 24 [n''(S)] to MO 13 [n'_σ(S)].

TABLE 2: Atomic Charges for the Molecular and Cation-Radical Forms of $CH_3C(O)SCH_3$ Calculated with the UB3LYP/6-311++G Approximation**[a]

	H_1	C_2	C_3	S_4	C_5	H_6	H_7	H_8	H_9	H_{10}	O_{11}	TAC[c]
$CH_3C(O)SCH_3$	0.152	−0.589	0.181	0.084	−0.452	0.158	0.176	0.176	0.172	0.172	−0.229	0
$CH_3C(O)SCH_3^+$	0.216	−0.712	0.386	0.536	−0.566	0.238	0.236	0.216	0.250	0.238	−0.038	+1
Δq[b]	0.064	−0.123	0.205	0.452	−0.114	0.08	0.06	0.04	0.078	0.066	0.191	+1

[a] For atom numbering, see Figure 2. [b] $\Delta q = q[CH_3C(O)SCH_3^+] - q[CH_3C(O)SCH_3]$. [c] Total atomic charge.

$CH_3C(O)SH$, and $CH_3C(O)SCH_2CH_3$ are 10.7, 10.0, and 9.6 eV, respectively.[40] Thus, the substitution of a hydrogen atom at sulfur by an electron-donating alkyl group results in a decrease of the ionization potential (IP).

The second ionization potential, observed at 9.81 eV, is assigned to the ionization process of an electron ejected from another predominantly nonbonding orbital, this time the n'(O) orbital. The following band, observed at 12.25 eV, is associated with ionizations from the π orbital of the carbonyl double bond. The three bands observed at 12.64, 13.17, and 14.63 eV are attributable to ionizations from the σ_{C-H} orbital of the CH_3 group directly bonded to the carboxylic carbon atom. The 15.23 eV feature in the PE spectrum is then linked to an ionization process from the σ_{C-H} orbital of the CH_3 group bonded to the S atom.

Calculations (UB3LYP/6-311++G**) were performed to analyze the nature of the cation formed in the first ionization process. The results demonstrate that the atomic charges are delocalized over the whole molecule, with an appreciable fraction localized at the S atom. As is evident from the details set out in Table 2, the partial positive charge of the S4 atom increases by 0.452 units (see also the characters of the first ionization process of Table 1 and of MO 24 in Figure 2). At the same time, the C3—S4 single bond experiences a marked elongation of about 0.36 Å, whereas the other bond lengths decrease. The lengthening of the (O)C—S bond is reflected even more conspicuously in the wavenumber of the mode approximating the ν(C—S) motion, which is calculated to fall to 231 cm^{-1}, as compared with the value of 619 cm^{-1} estimated at the same level of theory for the corresponding mode of the neutral molecule. The calculations find support from experiments with matrix-isolated $CH_3C(O)SCH_3$ revealing an IR multiplet absorption at 618/624/628 cm^{-1} that is most plausibly identifiable with this mode.[20] According to the same calculations, the syn orientation of the C—O and S—C bonds is retained after ionization. The value of the adiabatic IP is 9.0 eV in the UB3LYP/6-311++G** approximation.

Photoionization Processes. For absorptions above the ionization threshold, the quantum yield for molecular ionization is quite likely to tend to unity; that is, for each photon absorbed, an ion is produced. Consequently, the detection of parent and fragment ions as a function of the incident photon energy (TIY) is a powerful method that complements absorption spectroscopy.[41] Thus, an increment in the total ion production is expected every time that the incident energy exceeds a particular ionization potential as defined in PES conditions; the magnitude of the increment depends on the cross section of the particular ionic state. As is well-known, however, a valence ionic state — even one outside the ground state's Franck—Condon region — can be resonantly populated using tunable synchrotron radiation throughout a transition from the ground electronic state to a neutral Rydberg state, followed by a subsequent autoionization process. Similar, but not identical, transition energies are therefore to be expected when PE and TIY spectra are compared. Moreover, the yield of each of the differently formed ions (partial ion yield spectra) affords information about the dissociation channels associated with particular ionic states.

The TIY spectrum of $CH_3C(O)SCH_3$ in the photon energy range of 12.0—20.0 eV is depicted in Figure 3. The region between 12.0 and 14.0 eV reveals a group of well-defined signals that can be separated into two vibronically resolved bands. The maximum of the first occurs at 12.82 eV with a value of $\nu_o = 912 \pm 43$ cm^{-1} (see Table 1 and the inset of Figure 3), whereas the maximum of the second band occurs at 13.27 eV ($\nu_o = 671 \pm 147$ cm^{-1}); these bands correlate with the features at 12.25 and 13.17 eV, respectively, in the PE spectrum.

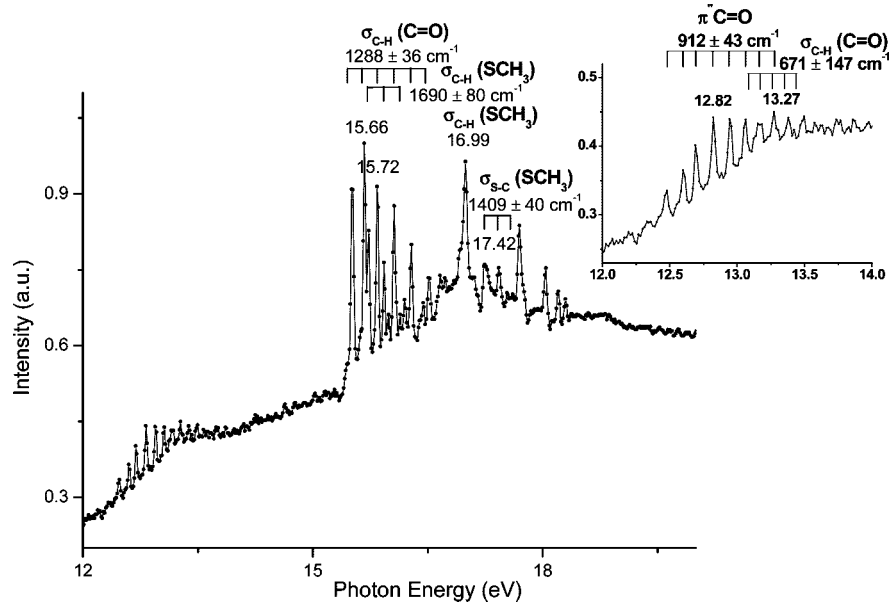

Figure 3. TIY spectrum of $CH_3C(O)SCH_3$ in the photon energy range 12.0−20.0 eV. The 12.0−14.0 eV region is enlarged in the inset on the right.

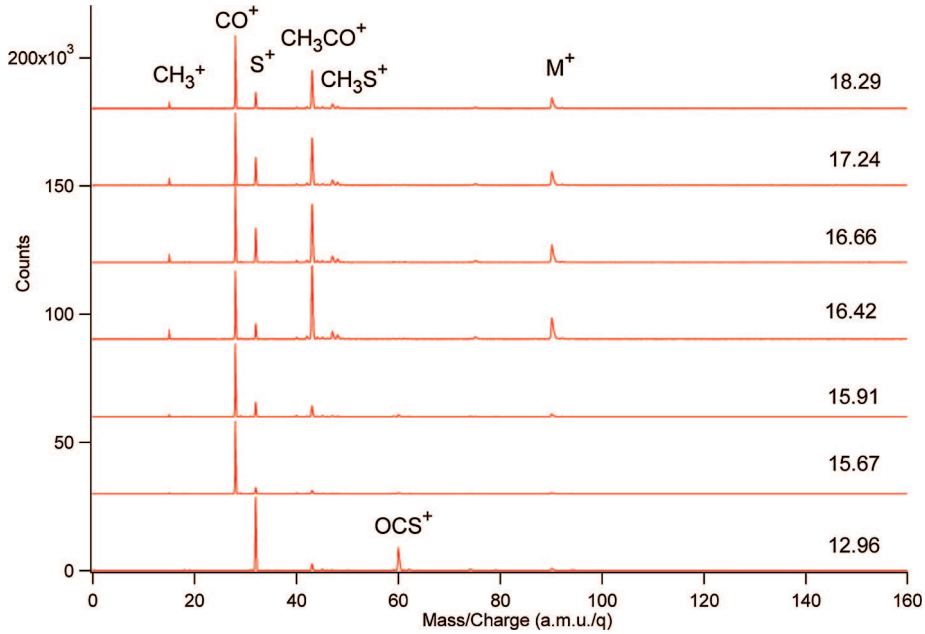

Figure 4. PEPICO spectra of $CH_3C(O)SCH_3$ at selected irradiation energies.

The next two bands at higher photon energy also display vibronic structure. The maxima are centered at 15.66 and 15.72 eV. The associated vibronic structure is characterized by $\nu_o = 1288 \pm 36$ cm^{-1} and $\nu_o = 1690 \pm 80$ cm^{-1}, respectively. The transition observed at 16.99 eV in the TIY spectrum correlates with the band near 15.23 eV in the PE spectrum of $CH_3C(O)SCH_3$. The next band in the TIY spectrum, located at 17.42 eV, is another showing well-defined vibronic structure with $\nu_o = 1409 \pm 40$ cm^{-1}. This transition can be assigned to an ionization involving the σ_{S-C} (SCH_3) orbital on the basis of the OVGF/6-311++G(d,p) calculations. The remaining transitions in the TIY spectrum, at 17.69 and 18.04 eV, can be identified with the σ_{S-C} (C═O) and n'_{σ}S orbitals, respectively.

The PEPICO spectra measured for $CH_3C(O)SCH_3$ at selected photon energies are shown, together with a fragment assignment of the bands, in Figure 4. The lowest energy delivered by the TGM beam line at the LNLS (12.0 eV) is higher than the first ionization potential of the $CH_3C(O)SCH_3$ molecule (9.5 eV). Accordingly, ionization processes from MO 24 and MO 23 (Table 1) can already be observed at the very first stage of the experiment. The PEPICO spectrum measured near 12.96 eV contains several signals. One weak signal corresponds to the parent molecular ion (M^+) (90 amu/q); others correspond to the fragments OCS^+ (60 amu/q), CH_3CO^+ (47 amu/q), and S^+ (32 amu/q). At this energy, a major contribution of the S^+ ion is observed in consonance with the first ionization process described in the preceding section. At photon energies near 15.67 and 15.91 eV, the ionization channel for the formation of CO^+ (28 amu/q) is opened, and this becomes the dominant fragment, accompanied by minor quantities of S^+ and CH_3CO^+. Depletion in the OCS^+ and S^+ fragments is evident from a comparison with the spectrum recorded at 12.96 eV. Again, such a finding is in agreement with the ionization processes occurring in this energy range, as listed in Table 1. Irradiation of $CH_3C(O)SCH_3$

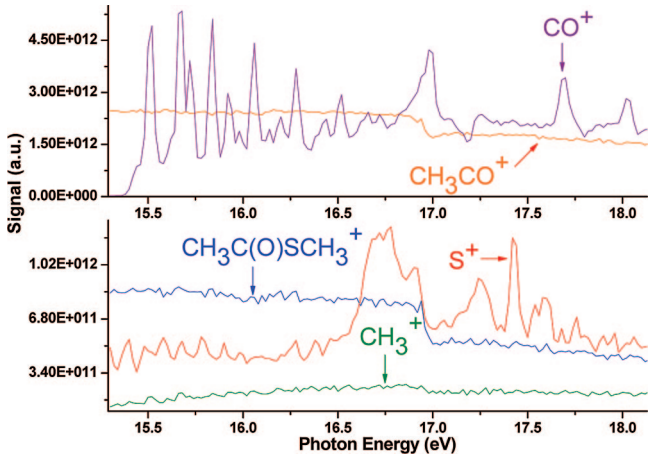

Figure 5. Partial ion yield (PIY) spectra of $CH_3C(O)SCH_3$.

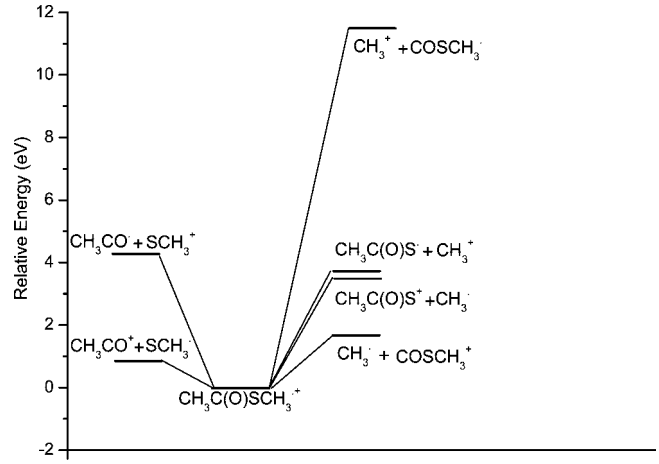

Figure 6. Energy profiles for dissociation of the molecular ion $CH_3C(O)SCH_3^+$.

with photons of increasing energy, namely, 16.42, 16.66, 17.24, and 18.29 eV, leads to a marked enhancement in the intensity of the signals corresponding to the CH_3CO^+ and $CH_3C(O)SCH_3^+$ ions. At these energies, access is gained to ionization channels for the production of the ions CH_3S^+ ($m/z = 47$ amu/q) and CH_3^+ ($m/z = 15$ amu/q) from ionized states of $CH_3C(O)SCH_3$. Many ionization processes are now attainable, and analysis of the individual fragments becomes more complicated.

A weak band at $m/z = 75$ amu/q is also observed. This signal is assigned to the loss of a CH_3 group from the parent molecular ion ($M^+ - 15$). The resulting ion can originate from the rupture of either the C—CH_3 or the S—CH_3 single bond of $CH_3C(O)SCH_3$.

In the electron-impact mass spectrum of $CH_3C(O)SCH_3$ measured at an ionization energy of 70 eV, the acylium ion, CH_3CO^+, with $m/z = 43$ amu/q, represents the most important product. The molecular ion $CH_3C(O)SCH_3^+$ also makes a significant contribution (23%). Other fragments, such as SCH_3^+ and HCS^+, show relative abundances on the order of 10%.[42]

More detailed information about the ion branching options can be gained from the partial ion yield (PIY) spectra shown for selected ions in Figure 5. These very time-consuming spectra were accumulated in the range of 15.3−18.1 eV by recording the count rates of selected ions as the photon energy was scanned in steps of 0.02 eV. Each point in a given PIY spectrum, which is normalized by the photon flux, corresponds to one TOF spectrum measured at this defined photon energy. The intensity of the signal corresponding to each ionic fragment was estimated by fitting a Gaussian function to the TOF spectra. It should be noted that the production of fragment ions might or might not coincide exactly with the ionization energy identified in the PE spectrum. If the ionic state has a dissociation channel giving direct access to the observed fragment ion, however, identical ionization energies should be observed.

The patterns of both the PIY spectrum of CO^+ and the TIY spectrum of $CH_3C(O)SCH_3$ are quite similar at the photon energies where the CO^+ and CH_3CO^+ ions are the predominant products. Irradiation of $CH_3C(O)SCH_3$ with photons at energies near 17.4 eV leads to the formation of S^+ ions.

Quantum chemical calculations were performed to estimate the energies of different pathways involving dissociation of the parent ion. A schematic representation of some of these dissociation channels is given in Figure 6. For the rupture of the C—S bond involving the carbonyl carbon atom, the calculations predicted that the channel affording $CH_3CO^+ +$ $^{\bullet}SCH_3$ is favored over that affording $CH_3CO^{\bullet} + SCH_3^+$. This is in agreement with the behavior observed in the PEPICO spectra, where CH_3CO^+ already appears at 12.96 eV, whereas much higher energies are needed to form the SCH_3^+ ion. The loss of a $^{\bullet}CH_3$ group from $CH_3C(O)SCH_3^{\bullet+}$ can produce either $CH_3C(O)S^+$ or $C(O)SCH_3^+$ ions ($m/z = 75$), with the latter being calculated to be energetically preferred. Similar bond ruptures leading to the formation of CH_3^+ are energetically more disadvantaged, especially the channel yielding $CH_3^+ +$ $^{\bullet}C(O)SCH_3$, which differs by approximately 9 eV from that yielding $^{\bullet}CH_3 + C(O)SCH_3^+$.

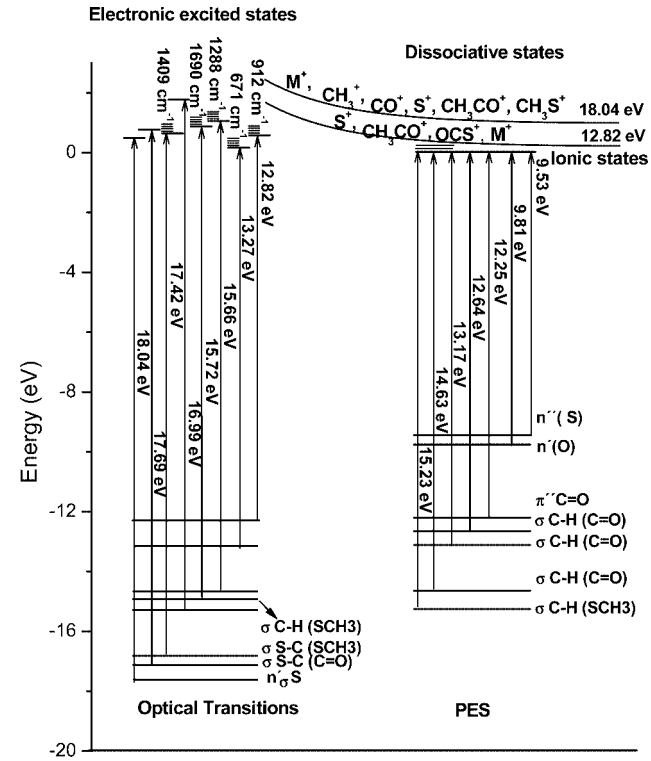

Figure 7. Schematic representation of the processes involved in the valence synchrotron photoionization and photoelectron spectra of $CH_3C(O)SCH_3$. Multiple levels of the excited state indicate vibronically resolved transitions.

Vibronic Structure. The features observed in the TIY spectrum in the synchrotron experiments include resonant excitations to neutral molecular states in addition to excitations marking photoionization processes, and it is the resonant

excitations that display vibronic structure. For instance, a resonant (optical) transition featuring vibronic structure occurs at 12.82 eV. At this energy, photoionization processes related to lower-energy events are also observed. We believe that the transitions to excited molecular states can be observed because the states are related to dissociative surfaces that lead to rupture of the molecule with the production of the ionic fragments detected.

The fine structure developed by each of five of the optical transitions in the TIY spectrum provides a selective vibrational view of the relevant excited electronic state of the $CH_3C(O)SCH_3$ molecule. The interpretation of this vibronic structure is, however, complicated by a number of factors. First, the parent molecule and its excited state have only low symmetry (C_s at best), and at wavenumbers below about 1500 cm^{-1}, few of their numerous vibrational modes are well described in terms of a single normal coordinate. Although it is reasonable to expect that the most prominent component of each vibrational progression is due to a vibrational transition that suffers a major change of wavenumber as a result of the transition in question, the relatively modest resolution of our spectra might well conceal more than one progression, nor does it follow that the interval in the progression is necessarily the wavenumber of a single fundamental vibration of the electronic excited state. Nevertheless, the vibronic structure can, in principle, provide important clues to the nature of that state and to the ionization process with which it is associated.

The lowest-energy optical transition for which such structure can be discerned, that at 12.82 eV, corresponding to the 12.25 eV feature in the PE spectrum signaling ionization from a $\pi''_{C=O}$ molecular orbital. The structure is dominated by a progression with $\nu_o = 912$ cm^{-1}. In the absence of more positive information, it is possible that the interval represents a vibrational mode of this particular excited electronic state of $CH_3C(O)SCH_3$ involving, at least in part, the ν(C═O) vibration. It would then signal a dramatic reduction in bond order of the original C═O bond brought about by the electronic promotion, with a corresponding decrease in the force constant and wavenumber of the C═O stretching vibration. By contrast, the ν(C═O) mode of the matrix-isolated parent molecule occurs as 1702/1709 cm^{-1}.[20] If our interpretation is correct, then the excited electronic state would appear justifiably to be represented by the structural formula **I** with a pyramidal framework. Moving to higher energy, the next three transitions to show vibronic structure in the optical spectrum correlate with ionization from σ_{C-H} orbitals of one or another of the CH_3 groups. It is now more difficult to anticipate how electronic excitation will affect the vibrational properties of the molecule. Whereas some bonds, such as C—H, will surely be weakened, others might well be strengthened by the redistribution of charge accompanying electronic excitation, and changes of polarity might mean that bending modes are as susceptible as any other modes to a major change of force constant. On the basis of the vibrational properties of the neutral molecule,[20] the progression with $\nu_o = 671$ cm^{-1} could correspond to a mode of the excited state with significant ν(C—S) character. Similarly, the progression with $\nu_o = 1288$ cm^{-1} can be tentatively identified with a vibrational fundamental in which $\delta(CH_3)$ is the dominant motion, whereas $\nu_o = 1690$ cm^{-1} is strongly suggestive of a ν(C═O) mode. Highest in energy of the transitions showing vibronic structure is that associated with ionization from a σ_{S-C} orbital associated with the S—CH_3 fragment of $CH_3C(O)SCH_3$. This progression is characterized by $\nu_o = 1409$ cm^{-1}, a wavenumber again hinting at what is mainly a $\delta(CH_3)$ vibration. Ideally, however, further experiments involving, for example, similar studies of perdeuterated S-methyl thioacetate, $CD_3C(O)SCD_3$, are needed to test this preliminary analysis.

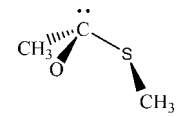

I

Conclusions

This study on the photoionization of the $CH_3C(O)SCH_3$ molecule has drawn on valence synchrotron photoionization and photoelectron data complemented with the results of quantum chemical calculations. It has enabled us to establish a schematic view of the optical and ionic transitions of S-methyl thioacetate, their correlation, and the photoproducts following an autoionization process. In this case, it has also yielded information about the electronic excited states through the media of several vibronic progressions that could be resolved in the TIY spectrum recorded in the synchrotron experiments. Figure 7 illustrates the states and transitions that have been identified.

References and Notes

(1) Ott, A.; Fay, L. B.; Chaintreau, A. *J. Agric. Food Chem.* **1997**, *45*, 850–858.

(2) Lamberet, G.; Auberger, B.; Bergère, J. L. *Appl. Microbiol. Biotechnol.* **1997**, *47*, 279–283.

(3) Lamberet, G.; Auberger, B.; Bergère, J. L. *Appl. Microbiol. Biotechnol.* **1997**, *48*, 393–397.

(4) Mestres, M.; Busto, O.; Guasch, J. *J. Chromatogr. A* **2000**, *881*, 569–581.

(5) Berger, C.; Khan, J. A.; Molimard, P.; Martin, N.; Spinnler, H. E. *Appl. Environ. Microbiol.* **1999**, *65*, 5510–5514.

(6) Helinck, S.; Spinnler, H. E.; Parayre, S.; Dame-Cahagne, M.; Bonnarme, P. *FEMS Microbiol. Lett.* **2000**, *193*, 237–241.

(7) Arfi, K.; Spinnler, H.; Tache, R.; Bonnarme, P. *Appl. Microbiol. Biotechnol.* **2002**, *58*, 503–510.

(8) Della Védova, C. O.; Romano, R. M.; Oberhammer, H. *J. Org. Chem.* **2004**, *69*, 5395–5398.

(9) Erben, M. F.; Boese, R.; Della Védova, C. O.; Oberhammer, H.; Willner, H. *J. Org. Chem.* **2006**, *71*, 616–622.

(10) Ulic, S. E.; Della Védova, C. O.; Hermann, A.; Mack, H. G.; Oberhammer, H. *Inorg. Chem.* **2002**, *41*, 5699–5705.

(11) (a) Idoux, J. P.; Hwang, P. T. R.; Hancock, C. K. *J. Org. Chem.* **1973**, *38*, 4239–4243. (b) Yang, W.; Drueckhammer, D. G. *J. Am. Chem. Soc.* **2001**, *123*, 11004–11009. (c) Yang, W.; Drueckhammer, D. G. *Org. Lett.* **2000**, *2*, 4133–4136.

(12) Summary of Evaluations Performed by the Joint FAO/WHO Expert Committee on Food Additives; Report TRS 896-JECFA 53/32; Compendium Addendum 8/FNP 52 Add.8/150; Tox monograph FAS 44-JECFA 53/125; ILSI Press: Washington, D.C., 2000.

(13) Arndt, F.; Loewe, L.; Ozansoy, M. *Ber. Dtsch. Chem. Ges.* **1939**, *72B*, 1862–1865.

(14) Suzuki, S.; Hisamichi, K.; Endo, K. *Heterocycles* **1993**, *35*, 895–900.

(15) El-Assar, A. M. M.; Nash, C. P.; Ingraham, L. L. *Biochemistry* **1982**, *21*, 1972–1976.

(16) Middaugh, R. L.; Drago, R. S. *J. Am. Chem. Soc.* **1963**, *85*, 2575–2576.

(17) Hilal, R.; El-Aaser, A. M. *Biophys. Chem.* **1985**, *22*, 145–150.

(18) Deerfield II, D. W.; Pedersen, L. G. *J. Mol. Struct. (THEOCHEM)* **1995**, *358*, 99–106.

(19) Nagy, P. I.; Tejada, F. R.; Sarver, J. G.; Messer, W. S., Jr. *J. Phys. Chem. A* **2004**, *108*, 10173–10185.

(20) Romano, R. M.; Della Védova, C. O.; Downs, A. J. *J. Phys. Chem. A* **2002**, *106*, 7235–7244.

(21) Erben, M. F.; Romano, R. M.; Della Védova, C. O. *J. Phys. Chem. A* **2004**, *108*, 3938–3946.

(22) (a) Geronés, M.; Erben, M. F.; Romano, R. M.; Della Védova, C. O. *J. Electron Spectrosc. Relat. Phenom.* **2007**, *155*, 64–69. (b) Gerones, M.; Erben, M. F.; Romano, R. M.; Della Védova, C. O.; Yao, L.; Ge, M. *J. Phys. Chem. A* **2008**, *112*, 2228–2234.

(23) Erben, M. F.; Romano, R. M.; Della Védova, C. O. *J. Phys. Chem. A* **2005**, *109*, 304–313.

(24) Erben, M. F.; Geronés, M.; Romano, R. M.; Della Védova, C. O. *J. Phys. Chem. A* **2006**, *110*, 875–883.

(25) Erben, M. F.; Geronés, M.; Romano, R. M.; Della Védova, C. O. *J. Phys. Chem. A* **2007**, *111*, 8062–8071.

(26) Lira, A. C. Rodrigues, A. R. D. Rosa, A. Gonçalves da Silva, C. E. T. Pardine, C. Scorzato, C. Wisnivesky, D. Rafael, F. Franco, G. S. Tosin, G. Lin Jahnel, L. Ferreira, M. J. Tavares, P. F. Farias, R. H. A. Neuenschwander, R. T. in *European Particle Accelerator Conference(Ed.: EPAC)*, Estocolmo, 1998.

(27) de Fonseca, P. T.; Pacheco, J. G.; Samogin, E.; de Castro, A. R. B. *Rev. Sci. Instrum.* **1992**, *63*, 1256–1259.

(28) Naves de Brito, A.; Feifel, R.; Mocellin, A.; Machado, A. B.; Sundin, S.; Hjelte, I.; Sorensen, S. L.; Bjorneholm, O. *Chem. Phys. Lett.* **1999**, *309*, 377–385.

(29) Cavasso Filho, R. L.; Homem, M. G. P.; Landers, R.; Naves de Brito, A. *J. Electron Spectrosc. Relat. Phenom.* **2005**, *144147*, 1125–1127.

(30) (a) Cavasso Filho, R. L.; Lago, A. F.; Homem, M. G. P.; Pilling, S.; Naves de Brito, A. *J. Electron Spectrosc. Relat. Phenom.* **2007**, *156158*, 168–171. (b) Filho, R. L. C.; Homen, M. G. P.; Fonseca, P. T.; Naves de Brito, A. *Rev. Sci. Instrum.* **2007**, *78*, 115104–115108.

(31) Zeng, X. Q.; Ge, M.; Sun, Z.; Bian, J.; Wang, D. *J. Mol. Struct.* **2007**, *840*, 59–65.

(32) Zeng, X. Q.; Yao, L.; Wang, W. G.; Liu, F. Y.; Sun, Q.; Ge, M. F.; Sun, Z.; Zhang, J. P.; Wang, D. X. *Spectrochim. Acta A* **2006**, *64*, 949–955.

(33) Yao, L.; Zeng, X. Q.; Ge, M. F.; Wang, W. G.; Sun, Z.; Du, L.; Wang, D. X. *Eur. J. Inorg. Chem.* **2006**, 2469–2475.

(34) Zeng, X. Q.; Liu, F. Y.; Sun, Q.; Ge, M. F.; Zhang, J. P.; Ai, X. C.; Meng, L. P.; Zheng, S. J.; Wang, D. X. *Inorg. Chem.* **2004**, *43*, 4799–4801.

(35) Wang, W.; Yao, L.; Zeng, X.; Ge, M.; Sun, Z.; Wang, D.; Ding, Y. *J. Chem. Phys.* **2006**, *125*, 234303–234306.

(36) Li, Y. M.; Zeng, X. Q.; Sun, Q.; Li, H. Y.; Ge, M. F.; Wang, D. X. *Spectrochim. Acta A* **2007**, *66*, 1261–1266.

(37) Wang, W. G.; Ge, M. F.; Yao, L.; Zeng, X. Q.; Sun, Z.; Wang, D. X. *ChemPhysChem* **2006**, *7*, 1382–1387.

(38) Cederbaum, L. S.; Domcke, W. *Adv. Chem. Phys.* **1977**, *36*, 205–344.

(39) Frisch, M. J.; Trucks, G. W.; Schlegel, H. B.; Scuseria, G. E.; Robb, M. A.; Cheeseman, J. R.; Montgomery, J. A., Jr.; Vreven, T.; Kudin, K. N.; Burant, J. C.; Millam, J. M.; Iyengar, S. S.; Tomasi, J.; Barone, V.; Mennucci, B.; Cossi, M.; Scalmani, G.; Rega, N.; Petersson, G. A.; Nakatsuji, H.; Hada, M.; Ehara, M.; Toyota, K.; Fukuda, R.; Hasegawa, J.; Ishida, M.; Nakajima, T.; Honda, Y.; Kitao, O.; Nakai, H.; Klene, M.; Li, X.; Knox, J. E.; Hratchian, H. P.; Cross, J. B.; Adamo, C.; Jaramillo, J.; Gomperts, R.; Stratmann, R. E.; Yazyev, O.; Austin, A. J.; Cammi, R.; Pomelli, C.; Ochterski, J. W.; Ayala, P. Y.; Morokuma, K.; Voth, G. A.; Salvador, P.; Dannenberg, J. J.; Zakrzewski, V. G.; Dapprich, S.; Daniels, A. D.; Strain, M. C.; Farkas, O.; Malick, D. K.; Rabuck, A. D.; Raghavachari, K.; Foresman, J. B.; Ortiz, J. V.; Cui, Q.; Baboul, A. G.; Clifford, S.; Cioslowski, J.; Stefanov, B. B.; Liu, G.; Liashenko, A.; Piskorz, P.; Komaromi, I.; Martin, R. L.; Fox, D. J.; Keith, T.; Al-Laham, M. A.; Peng, C. Y.; Nanayakkara, A.; Challacombe, M.; Gill, P. M. W.; Johnson, B.; Chen, W.; Wong, M. W.; Gonzalez, C.; Pople, J. A. *Gaussian 03*, revision B.04; Gaussian, Inc.: Pittsburgh, PA, 2003.

(40) (a) Nagata, S.; Yamabe, T.; Fukui, K. *J. Phys. Chem.* **1975**, *79*, 2335–2340. (b) Erben, M. F.; Della Védova, C. O. *Inorg. Chem.* **2002**, *41*, 3740–3748.

(41) Nenner, I. Beswick, J. A. In *Handbook on Synchrotron Radiation*; Marr, G. V. Ed.; Elsevier Science Publishers: New York, 1987; Vol. 2, pp 355−462.

(42) Linstrom, P. J., Mallard, W. G. Eds. NIST Standard Reference Database Number 69; National Institute of Standards and Technology: Gaithersburg, MD, 2003; available at http://webbook.nist.gov.

JP801295G